Journal of Alloys and Compounds 503 (2010) 163–169

Contents lists available at ScienceDirect

Journal of Alloys and Compounds

journal homepage: www.elsevier.com/locate/jallcom

Lateral parameter variations on the properties of $La_{0.7}Sr_{0.3}MnO_3$ films prepared on Si (1 0 0) substrates by dc magnetron sputtering

Dipti Ranjan Sahu [a,b,*]

[a] Institute of Materials Science, Bhubaneswar 751013, India
[b] School of Physics, University of the Witwatersrand, Private Bag 3, Wits 2050, Johannesburg, South Africa

ARTICLE INFO

Article history:
Received 9 September 2009
Received in revised form 29 April 2010
Accepted 30 April 2010
Available online 6 May 2010

PACS:
75.50.Kj
75.70.Pa
75.30.Vn
75.70.−I
75.30 Gw

Keywords:
CMR
LSMO
Sputtering
Electrical and magnetic properties

ABSTRACT

$La_{0.7}Sr_{0.3}MnO_3$ (LSMO) is an interesting colossal magnetoresistance material for application in electronic and spintronics devices. A phenomenon in the planner magnetron sputtering of the LSMO films that is not well investigated as yet are the laterally non-uniform film properties resulting from the laterally inhomogeneous erosion of the target material, whereby the lateral distribution of the film properties depend strongly on the deposition parameters. The lateral distributions of the electrical, magnetic and structural properties of LSMO films prepared by dc magnetron sputtering on Si substrates are investigated across a distance of 64 mm using four-point probe, vibrating sample magnetometer and X-ray diffraction. In room temperature the T_{MI} and T_c of this film without any additional buffer layer are 245 K and 325 K, respectively, which makes them very interesting as spin source in Si based technology. Hence, it seems that sputter deposited LSMO is a promising CMR materials for spintronics devices.

1. Introduction

$La_{0.7}Sr_{0.3}MnO_3$ (LSMO) a representative manganites which shows colossal magnetoresistance (CMR) have attracted great research interest as an advanced material for potential spintronic applications [1–8]. A variety of deposition techniques, including pulsed laser deposition [9–11], sputtering [12,13], MOCVD [14,15], metal–organic decomposition [16], laser ablation [17], chemical coprecipitation [18], molecular beam epitaxy [19], etc. have been employed for the growth of LSMO on different substrates. However, special interest is the magnetron sputtering because of its low cost, high stability against hydrogen plasma and heat cycling that grows at low temperature and has good properties. In addition sputtering of LSMO has relatively high deposition rate and hence is well suited to industrial-scale large area deposition [20]. Different substrates such as $SrTiO_3$ (STO), $LaAlO_3$, $NdGaO_3$, MgO, Sapphire and Silicon are employed for the growth of high quality manganites thin film [21–24]. But for economical reason and industrial applications low cost Si substrates are preferable [25]. Although perovskite manganite thin films have been successfully grown on expensive single-crystal substrates such as $LaAlO_3$ and $SrTiO_3$, but successful growth and optimization of these films on silicon (Si) substrates is the essential materials for the semiconductor industry, are still needed.

Various articles exist in literature that investigates the dependence of the structural, electrical and magnetic properties of the sputtered LSMO films [26–31]. The characteristics of LSMO films are generally affected by the preparation conditions such as the deposition methods, working pressure, substrate temperature and the type of substrates [32]. However, detail investigation of film properties on the deposition parameter such as dc power, working pressure, substrate temperature, substrate-target distance, flow of argon and oxygen during sputtering are not well-studied so far.

In this present work, we have addressed this issue through detailed study of the effect of deposition parameter across the entire substrates on structural, magnetic, magnetoresistance (MR) specially its temperature and magnetic field dependence properties.

2. Experimental

A sintered oxide disk of LSMO (purity 99.99%, diameter 100 mm, thickness 3 mm) was used for the preparation of film on Si (1 0 0) substrate by dc sputtering. The tar-

* Correspondence address: School of Physics, University of the Witwatersrand, Private Bag 3, Wits 2050, Johannesburg, Guteng, South Africa. Tel.: +27 11 7176839; fax: +27 11 7176879.
E-mail address: Diptiranjan.Sahu@wits.ac.za.

0925-8388/$ – see front matter © 2010 Elsevier B.V. All rights reserved.
doi:10.1016/j.jallcom.2010.04.225

get was sintered to high density by conventional solid state sintering route using resistive heating (3 kW Al_2O_3 tube furnace operated at 1450 °C for 10 h). It may be noted that the density of the target is approximately 95% of the theoretical value. During deposition the vertical distance between the target disk and the Si substrate was about 80 mm. Before each deposition, a base pressure of 1.6×10^{-6} Torr was established using turbomolecular pump. The substrate was ultrasonically cleaned in acetone, rinsed in deionized water and subsequently dried in flowing nitrogen. During sputtering argon and oxygen flow rate, dc power, deposition time and substrate temperatures were varied. After deposition samples are cooled down to room temperature. Film thickness was measured using a surface profiler (Alpha step 500, TENCOR). The diffraction patterns of the films were recorded with the help of Philips PW 1917 X-ray powder diffractometer using CuK_α radiation. Electron probe microanalysis (EPMA) was used to check the chemical composition of the films. Magnetoresistance and electrical properties of LSMO was measured by four-point probe technique. The resistance of the target was about ≈1.265 Ω at room temperature before deposition of the film. The probe current was parallel to the longitudinal direction of sample and the magnetic field was parallel to the current direction. The magnetization was measured by vibrating sample magnetometer (VSM) within the range 100–300 K.

3. Results and discussion

3.1. General properties of fabricated films

3.1.1. Deposition rate

The deposition rate, measured at the central spot of the substrate (which correspond to the centre of the target disk), as a function of dc power at two working gas pressure and two substrate temperature is shown in Fig. 1(a), while the deposition rate versus Ar:O_2 gas phase composition is shown in Fig. 1(b) (in *X*-axis scale 2, 4, . . . , means Ar:O_2 is 2:8 and 4:6, etc.). It was observed for a given working gas pressure and substrate temperature that the deposition rate is found to be proportional to the dc power. At an Ar:O_2 gas phase composition of 7:3 (denoted as 7 in *X*-axis), the deposition rate was same for two investigated substrate temperature (650 °C and 700 °C). Furthermore, for both substrate temperatures, the deposition rate was observed to increases with decreasing of oxygen gas.

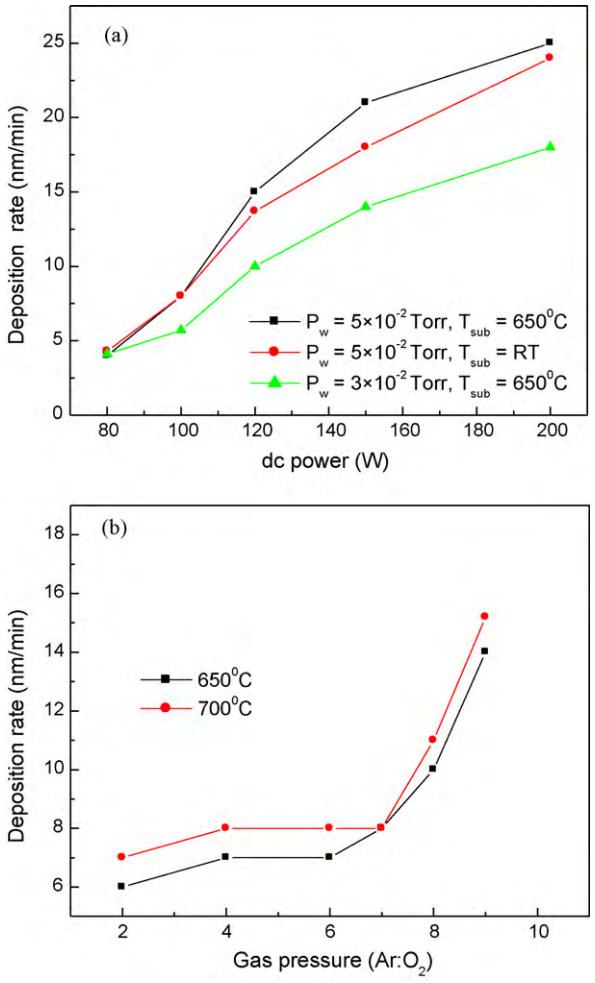

Fig. 1. The deposition rate versus (a) dc power (b) gas phase composition (Ar:O_2). The sputtering condition in plot (b) is P_{dc} = 100 W. The measurements were taken on the central region of the substrates.

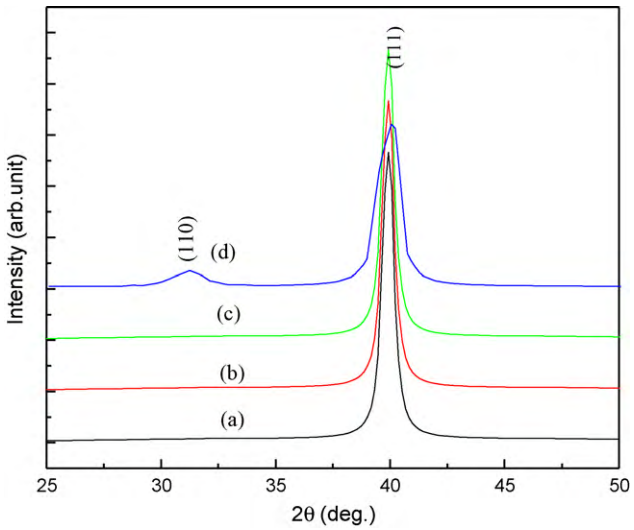

Fig. 2. The XRD pattern of the LSMO film deposited at $P_w = 5 \times 10^{-2}$ Torr, Ar:O_2 = 7:3, T_{sub} = 650 °C and various dc power P_{dc}: (a) 80 W, (b) 100 W, (c) 150 W. Also shown (d) is the XRD pattern of film deposited at $P_w = 5 \times 10^{-2}$ Torr, Ar:O_2 = 8:2, T_{sub} = 300 °C.

3.1.2. Structural properties

Fig. 2 shows the typical XRD pattern of LSMO film deposited at dc power of 80 W, 100 W and 150 W, respectively, using a working pressure of 5×10^{-2} Torr, Ar:O_2:7:3 and the substrate temperature 650 °C. For a comparison study, the XRD pattern of film prepared at higher Ar:O_2 pressure (8:2) having substrate temperature 300 °C is also included. The measurement was taken in the central region of the samples. Slow scanning was performed for proper peak resolution. After slow scanning and backward noise correction the enlarged view of the XRD patterns are shown in Fig. 2. The (1 1 1) peak is observed at a $2\theta = 40°$ for all samples. The observed increase in intensity with increasing dc power reveals that the increase of sputtering power improves the crystallinity of the film. The weak diffraction intensity and the appearance of (1 1 0) peak indicates that a higher Ar:O_2 gas phase composition and lower substrate temperature cause a degradation of the preferred orientation of the crystallinity. The composition of the films grown at 650 °C was confirmed by EPMA to be $La_{0.7}Sr_{0.3}MnO_{3-\delta}$. The elemental analysis shows that the LSMO layer is compositionally homogeneous and in spite of the high deposition temperature there is no evidence for diffusion of Si into the LSMO layer. On the other hand some local oxygen diffusion into the Si has been observed. Moreover, no signature of chemical reaction at the interface has been found. It is observed that grains size is increasing with increase of substrate temperature. At 300 °C the grain are not well-formed and distributed non-uniformly. But the grains are uniform and have well distribution with smooth surface at the deposition temperature 650 °C. The grain size could be change with the variation of dc power and working pressure and are within the range ≈25–30 nm. With further increase of substrate temperature or dc power grain growth takes place and coalescence of the islands seems to be happens from the increase of the size of grains.

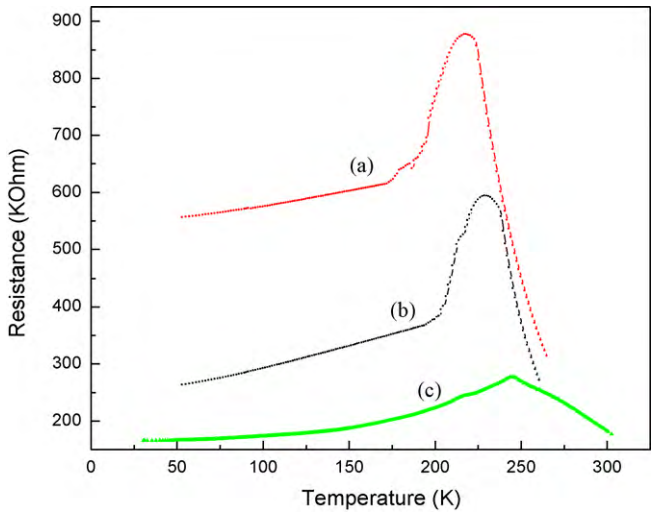

Fig. 3. The temperature dependent resistance in the central position of the substrates. The three sputtering conditions are (a) $P_w = 3 \times 10^{-2}$ Torr, $T_{sub} = RT$; (b) $P_w = 3 \times 10^{-2}$ Torr, $T_{sub} = 650\,^{\circ}C$; (c) $P_w = 5 \times 10^{-2}$ Torr, $T_{sub} = 650\,^{\circ}C$.

3.1.3. Electrical properties

The resistance of the fabricated LSMO films measured at the central spot of the substrate, as a function of temperature at different working gas pressure and substrate temperature is shown in Fig. 3. It is observed that the resistance of the film decreases and the metal insulator transition temperature (T_{MI}) increases with increase of substrate temperature. This can be explained by the effect of grain boundaries [33,34]. The grain was grown and the fraction of the grain boundaries in higher substrate temperature was increased to enhance the connectivity among the grains. Therefore, as the substrate temperature increased, the resistance of films decreased. The power range in which the films exhibit lower resistance and higher T_{MI} is different for the given three curves in Fig. 3. For substrate temperature (T_{sub}) = 650 °C, the optimum power reduces from 150 W to 100 W, when the working gas pressure increases from 3×10^{-2} Torr to 5×10^{-2} Torr. The highest T_{MI} of 245 K is achieved for the following sputtering parameters: working pressure (P_w) = 5×10^{-2} Torr, dc power (P_{dc}) = 100 W and T_{sub} = 650 °C. This behavior of the resistance with dc power and T_{MI} of LSMO is in good agreement with the investigation at different annealing temperature and on different substrates by Du et al. [28]. So, it is concluded that machine related issues (deposition parameter, substrate position, substrate type, etc.) can affect the morphological structure and microscopic imperfection (grain boundaries, surface roughness, etc.) of the films. It is observed that T_{MI} of the film is different from the bulk. This may be caused by a higher degree of oxygen deficiency during synthesis of films inside the sputtering chamber or due to strain effect of the substrate [35–39].

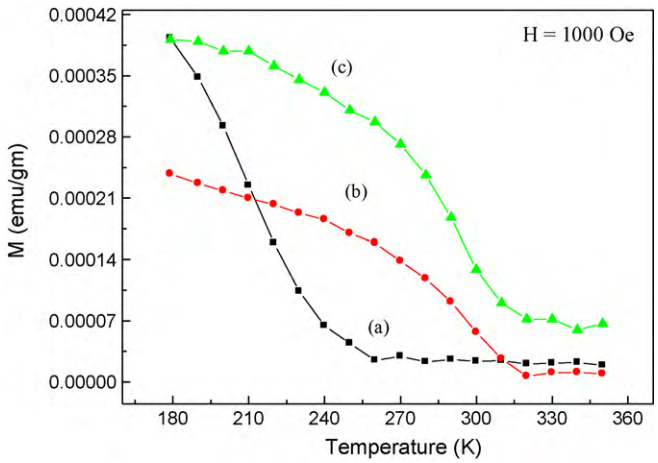

Fig. 4. Temperature dependent magnetization in the central position of the substrates. The three sputtering conditions are (a) $P_w = 3 \times 10^{-2}$ Torr, $T_{sub} = RT$; (b) $P_w = 3 \times 10^{-2}$ Torr, $T_{sub} = 650\,^{\circ}C$; (c) $P_w = 5 \times 10^{-2}$ Torr, $T_{sub} = 650\,^{\circ}C$.

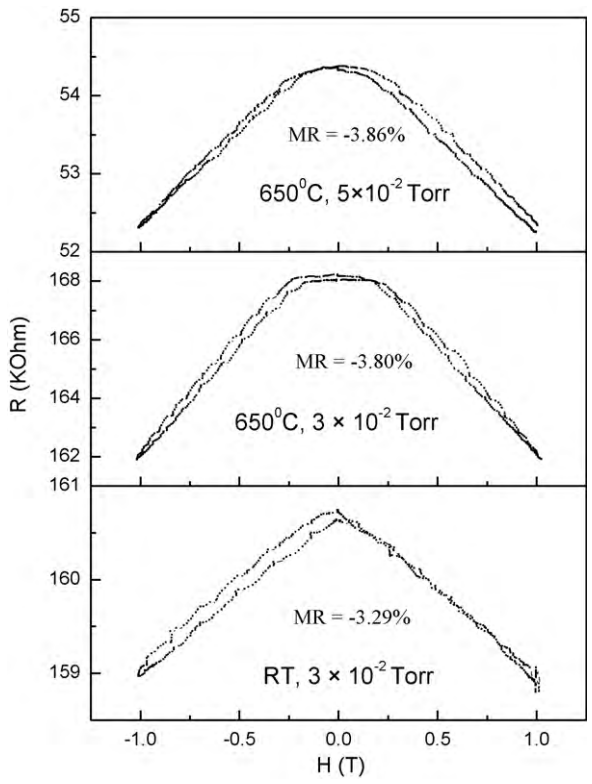

Fig. 5. The room temperature magnetoresistance as a function of H for LSMO films at different conditions of working gas pressure and substrate temperature.

3.1.4. Magnetic properties

Fig. 4 shows the temperature dependence magnetization (M) curves for LSMO film with an applied field of 1000 Oe measured in

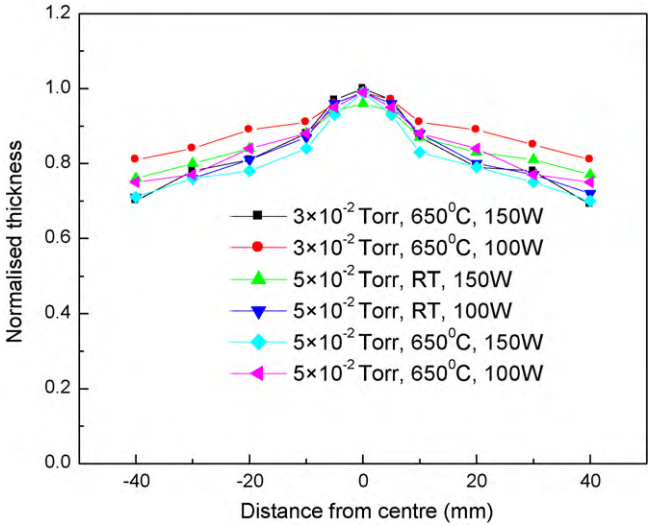

Fig. 6. The normalized lateral thickness distribution of the LSMO films made under different sputtering conditions (the parameters in the legand are P_w, T_{sub} and P_{dc}, respectively).

the central regions of substrates at different working gas pressure and substrate temperature. The Curie temperature is very small for the as grown films that increase with increase of substrate temperature. Magnetization also shows the same trend as that of R–T curve. Higher T_c of 325 K was observed at higher substrate temperature and at higher working pressure. However, T_c is always higher than that of T_{MI} for all the film. Difference in T_c and T_{MI} may be due to the formation of small ferromagnetic cluster, which are large enough to give a magnetic contribution but not to allow metallic conductivity appearing in zones of ferromagnetic insulating behavior [40]. The T_c value that is obtained is different than the reported values and is due to growth of the film on single-crystalline substrate, post-annealing or deposition of buffer layer before growing of LSMO film on Si or growth of the film by the different deposition methods [41–47]. In this work film was grown by dc sputtering on Si substrate without any buffer layer or post-annealing. Difference in the T_c value for this growth may be due to interface problems and change in the strain behaviors of the film and substrate. Films may be attributed to poor interface quality. The key lies in the engineering of the interface between the film and the substrate for the high value of T_c, grown with suitable deposition method [45]. It involves growing very high-quality single-crystalline film by tuning the growth temperature and post-annealing in oxygen ambient in order to relax the strain between the film and the substrate that improves the surface morphology. It is reported that the strains are controlled by the physical properties of the films [45,46]. Other possibilities are may be the oxygen non-stoichiometry at the LSMO/Si interface. The reduction in T_c is caused by the interface disorders. On the other hand, the surface morphology of the multilayered films is also influenced by the thickness of the films [47]. The presence of inhomogeneity, mostly at the interface, also significantly influences the magnetic properties. However, T_c value reported here is exactly same for the film grown on Si substrate by Bergenti et al. [48] using pulsed plasma deposition.

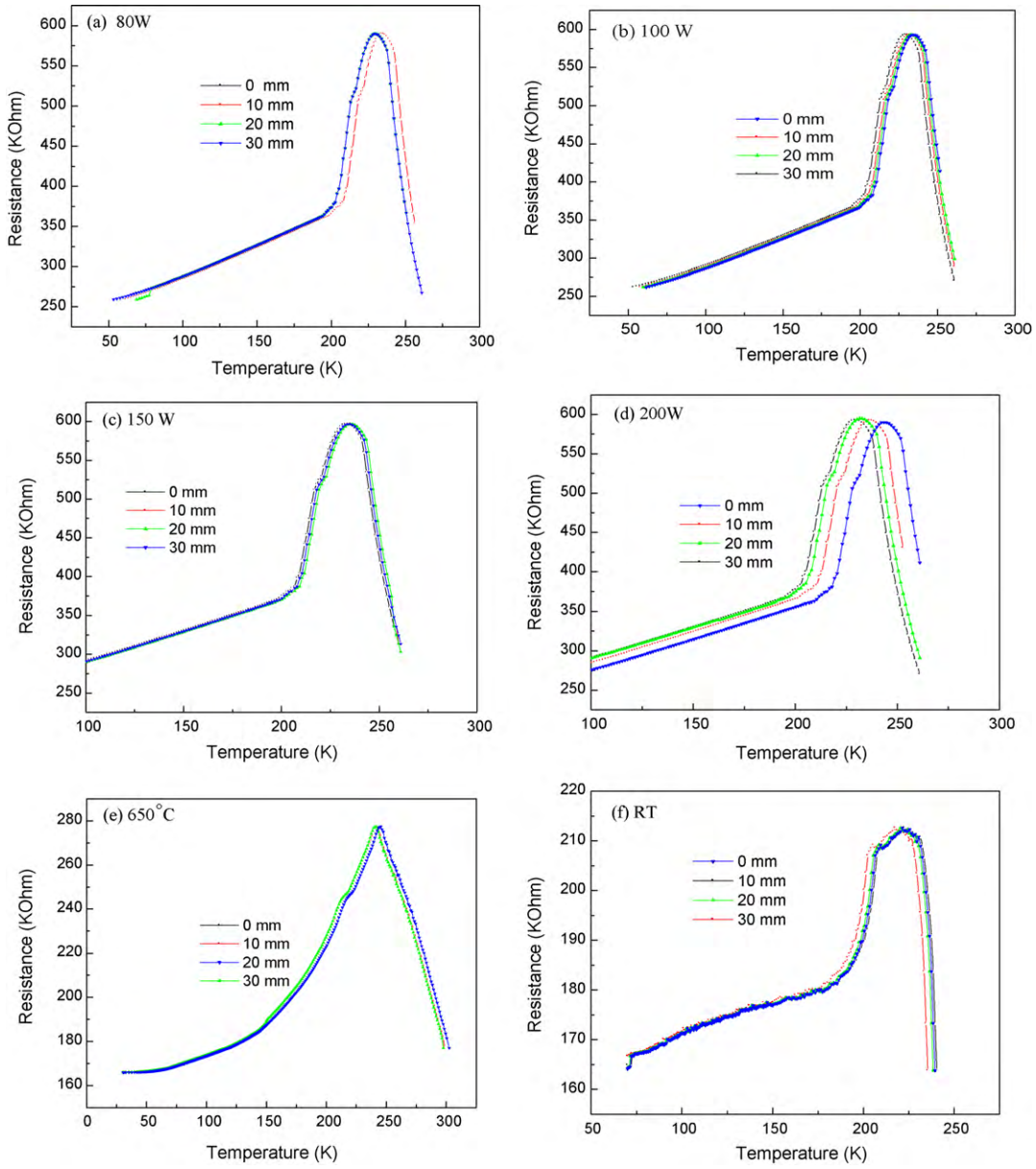

Fig. 7. The lateral distribution of resistance versus temperature of the LSMO films on Si made under different sputtering conditions. In plots (a)–(d), the, the working pressure and the substrate temperature are constant (3×10^{-2} Torr, 650 °C), while dc power has the following values: (a) 80 W, (b) 100 W, (c) 150 W, (d) 200 W. In plots (e) and (f) working pressure and dc power are constant (5×10^{-2} Torr and 100 W), while the substrate temperature has the following values (e) 650 °C and (f) *RT*. The number indicates in the legand for the curves are the position of the measured film (distance in mm) from the central position of the substrate.

3.1.5. Magnetoresistance

Fig. 5 presents the magnetoresistance curve (R–H) measured in the central regions of substrates at different working gas pressure and substrate temperature. Magnetoresistance ratio (MR) is defined as MR% = $[(R(H) - R(0))/R(0)]$ 100%, with $R(H)$ and $R(0)$ corresponding to electrical resistance at an external field of H and 0, respectively. It is found that magnetoresistance ratio increased with increase of substrate temperature. MR ratio up to −3.86% was observed on the film prepared at substrate temperature of 650 °C having working pressure of 5×10^{-2} Torr. At room temperature, the relation of MR with applied field is less linear, which suggest that there may be existence of some cavities in the film. The disordered long range magnetic domain could not overcome the thermal excitation, therefore it was disordered and caused less linear relationship between MR in an applied filed. However, MR–H curves can be divided into two stages for the film prepared at 650 °C substrate temperature. At low field up to 0.2 T MR curve is almost flat but MR–H curve becomes more linear when external field was increased. The magnetization could not reach saturation; therefore, the thermal excitation is also difficult to be overcome by an applied field of 1 T. The linear relationship of MR–H curve can be explained that the microstructure of grain domain in long range magnetic order is increased by increasing external applied field to lead the linear relationship between MR and H [49]. Furthermore, with decrease of measuring temperature MR increases, which is suggested to stem from spin dependent scattering of polarized electron at the grain boundaries [50]. It is noticeable that, the appearance of MR at room temperature would promote the application studies.

3.2. Lateral distribution of film properties

3.2.1. Thickness

The laterally inhomogenous erosion of the target material in magnetron sputtering results in a dependence of the film properties on the position on the substrate. In our system, the ring like erosion crater has a cross-sectional width of ~17 mm. The longer the target

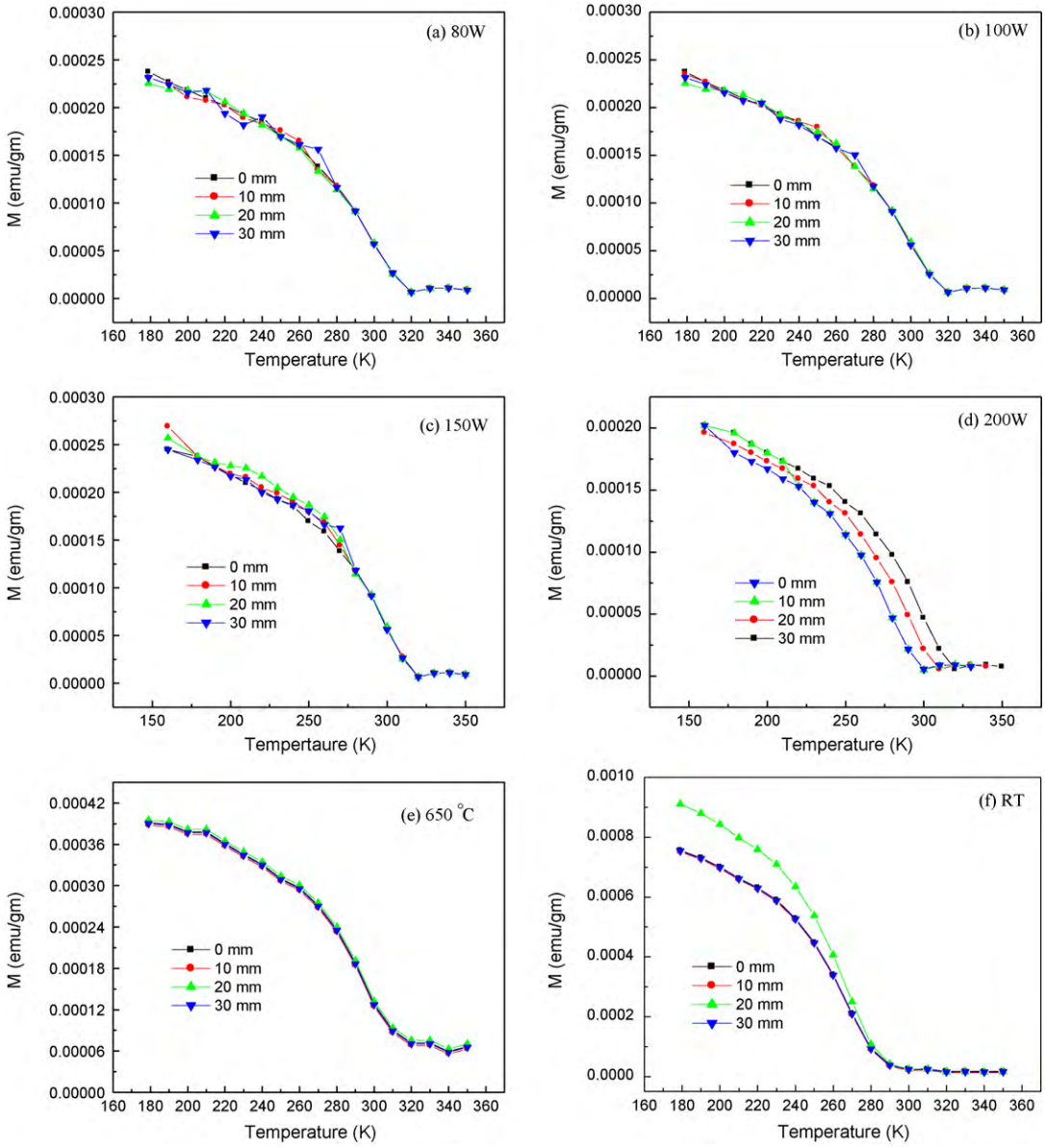

Fig. 8. The lateral distribution of magnetization versus temperature of the LSMO films on Si made under different sputtering conditions. In plots (a)–(d), the, the working pressure and the substrate temperature are constant (3×10^{-2} Torr, 650 °C), while dc power has the following values: (a) 80 W, (b) 100 W, (c) 150 W, (d) 200 W. In plots (e) and (f) working pressure and dc power are constant (5×10^{-2} Torr and 100 W), while the substrate temperature has the following values (e) 650 °C and (f) *RT*. The number indicates in the legand for the curves are the position of the measured film (distance in mm) from the central position of the substrate.

is used, the deeper and wider the erosion crater gets. The thickness of the LSMO film as a function of the distance from the central spot of the substrate (corresponding to the centre of the target disk) were investigated to find the possible correlation between the film properties, the sputtering parameter and distance from the central spot.

Fig. 6 shows the normalized film thickness distribution across the substrates obtained for different sputtering conditions. The zero in the figure corresponds to the central spot of the substrates or equivalently, the central spot of the target material. For all sputtering conditions, the thickness is maximal at the centre of the substrates and reduces towards its edges. The erosion crater has no significant impact on the thickness distribution of the films. The thickness of the film at the centre of the substrate is about 100 nm. The thickness variation across the entire substrates (measured distance = 64 mm) is smallest (±10%) for a low pressure (3×10^{-2} Torr) and high substrate temperature. For other investigated sputtering conditions the thickness variation is 15–20% across the entire substrates. This indicates that the surface mobility of sputtered particles is enhanced at higher T_{sub} and lower P_w.

3.2.2. Electrical and magnetic properties

Figs. 7 and 8 show the full dependence of the resistance and magnetization as a function of temperature for LSMO film on the sputtering condition and on the lateral position on the substrate (various curve in each individual plot). In plots (a)–(d) the working pressure and the substrate temperature are constant (3×10^{-2} Torr, 650 °C), while dc power has the values 80 W, 100 W, 150 W, 200 W, respectively. In plots (e)–(f) the working pressure (5×10^{-2} Torr and dc power 100 W) are constant, while the substrate temperature has the values 650 °C and *RT*. The position of the measured film spot (the distance in mm) on the substrates is indicated in the legand. The film prepared at 200 W dc power shows difference in the value of T_{MI} and T_c than the other films. However, for other films the lateral variation of the above properties is same as that of the central position of the film. As already mentioned the sputtering conditions have a very strong impact on the resistance and magnetization of the film. Figs. 7 and 8, furthermore shows that for certain sputtering condition, the films show significant lateral variations in their properties. The strongest lateral variations are observed for the sputtering conditions of power 200 W, $P_w = 3 \times 10^{-2}$ Torr and $T_{sub} = 650$ °C.

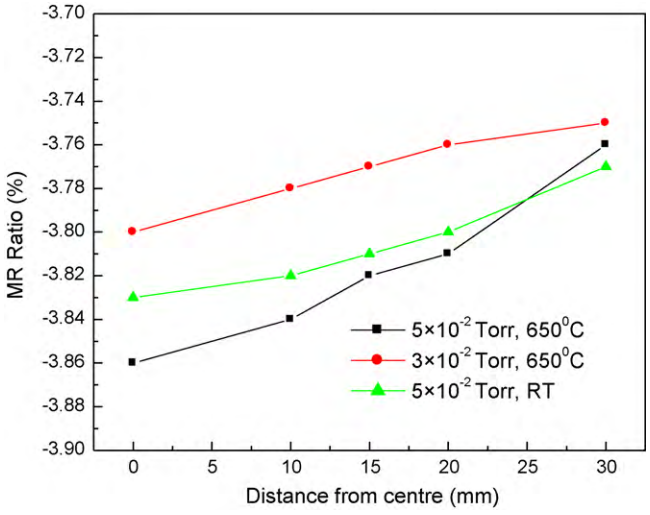

Fig. 9. Lateral variation of magnetoresistance ratio for LSMO film prepared at fixed $P_{dc} = 100$ W and with different working pressure and substrate temperature (the parameters in the legand are P_w and T_{sub}, respectively).

Fig. 9 presents the variation of MR ratio on the lateral position on the substrate. It is observed that there is marginal decrease of MR ratio with the position of the substrate. The central position of the substrate shows maximum MR ratio. Variation of small amount of MR may be due to small variation of T_c, which is happened due to marginal thickness difference of the film. The lateral variations of the parameters of the LSMO films prepared by dc magnetron sputtering can be reduced to acceptable levels by optimizing the deposition parameters.

4. Conclusions

The lateral distribution of the electrical and magnetic properties of the LSMO film prepared by the dc sputtering on Si substrates are investigated across a distance of 64 mm using four-point probe technique and magnetization measurements. At a given working pressure, the same growth rate is found at the substrate temperatures of 600–700 °C but growth rate is found to be inhomogenous across the substrates. The film thickness is maximal at the central region of the substrates (during sputtering process, is located below the centre of the target) and reduces with increasing distance from the centre. The lateral parameter variations are minimized using optimized sputtering conditions which are at low P_w and high T_{sub}. The particular parameter set ($P_w = 5 \times 10^{-2}$ Torr, $T_{sub} = 650$ °C and $P_{dc} = 100$ W) gives the most uniform electrical and magnetic property in this work. With this parameter, the film property at the central substrate region and lateral variation is rather small (±5%) and the property is uniform across the entire substrates. In room temperature the T_{MI} and T_c of these films without any additional buffer layer are 245 K and 325 K. Hence, LSMO film exhibiting CMR can be grown onto Si (1 0 0) without any buffer layer by DC magnetron sputtering that may be used as a promising material for large area spintronics devices.

Acknowledgement

Author is thankful to Director, Institute of Materials Science, Bhubaneswar for his encouragement and School of Physics, University of the Witwatersrand, Johannesburg, South Africa for supporting the research work.

References

[1] M.B. Salamon, M. Jaime, Rev. Mod. Phys. 73 (2001) 583.
[2] A.J. Millis, Nature (London) 392 (1998) 147.
[3] C.N. Rao, A.K. Cheetham, Science 276 (1997) 911.
[4] N.V. Volkov, E.V. Eremin, V.S. Tsikalov, G.S. Patrin, P.D. Kim, S.C. Yu, D.H. Kim, N. Chau, Tech. Phys. Lett. 35 (2009) 990.
[5] M. Kang, H.J. Kim, S. Yoo, Appl. Phys. Lett. 95 (2009) 052510.
[6] G.A. Ovsyannikov, A.M. Petrzhik, I.V. Borisenko, A.A. Klimov, Y.A. Ignatov, V.V. Demidov, S.A. Nikitov, J. Exp. Theor. Phys. 108 (2009) 48.
[7] G.M. Ren, S.L. Yuan, Z.M. Tian, Thin Solid Films 517 (2009) 3748.
[8] K. Kioka, T. Honma, T. Ishibashi, T. Komatsu, Solid State Commun. 149 (2009) 1795.
[9] R. Desfeux, S. Bailleul, A. Da Casta, W. Prelier, A.M. Haghiri-Gosnet, Appl. Phys. Lett. 78 (2001) 3681.
[10] M. Veis, S. Visnovskỹ, P. Lecoeur, A.-M. Haghiri-Gosnet, J.-P. Renard, P. Beauvillain, B. WPrellier, J. Mercey, T. Mistrĩik, Yamaguchi, J. Phys. D: Appl. Phys. 42 (2009) 195002.
[11] A.K. Pradhan, D.R. Sahu, B.K. Roul, Y. Feng, J. Appl. Phys. 96 (2004) 1170.
[12] Y. Luo, A. Kaufler, K. Samwer, Appl. Phys. Lett. 74 (2000) 87.
[13] M. Spankova, S. Chromik, I. Vavra, V. Strbik, J. Liday, P. Vogrincic, J.P. Espinos, P. Lobotka, Phys. Status Solidi A 206 (2009) 1456.
[14] S. Pignard, H. Vincent, J.P. Senateur, P.H. Giauque, Thin Solid Films 347 (1999) 161.
[15] L. Meda, K.H. Dahmen, S. Hayek, H. Garmestani, J. Cryst. Growth 263 (2004) 185.
[16] X. Zhu, H. Shen, Z. Tang, K. Tsukamoto, T. Yanagisawa, M. Okutomi, N. Higuchi, J. Alloys Compd. 488 (2009) 437.
[17] I.T. Gomes, B.G. Almeida, A.M.L. Lopes, J.P. Araujo, J. Barbosa, J.A. Mendes, J. Magn. Magn. Mater. 322 (2010) 1174.
[18] Z.F. Zi, Y.P. Sun, X.B. Zhu, C.Y. Hao, X. Luo, Z.R. Yang, J.M. Dai, W.H. Song, J. Alloys Compd. 477 (2009) 414.

[19] Z. Yang, L. Sun, C. Ke, X. Chen, W. Zhu, O. Tan, J. Cryst. Growth 311 (2009) 3289.
[20] E.S. Vlakhov, T.I. Donchev, A.Y. Spasov, K. Dorr, K.A. Nenkov, A. Handstein, S. Pignard, H. Vincent, Vacuum 69 (2003) 149.
[21] H. Boschker, M. Mathews, E.P. Houwman, H. Nishikawa, A. Vailionis, G. Koster, G. Rijnders, D.H.A. Blank, Phys. Rev. B 79 (2009) 214425.
[22] Y.M. Kang, N.A. Ulyanov, G.M. Shin, S.Y. Lee, D.G. Yoo, S.I. Yoo, J. Appl. Phys. 105 (2009), p. 07D711.
[23] X. Tan, K. Jin, S.G. Zhao, C.L. Chen, Rare Met. Mater. Eng. 38 (2009) 168.
[24] Z. Konstantinović, Ll. Balcells, B. Martínez, J. Magn. Magn. Mater. 322 (2010) 1205.
[25] E. Steinbeib, K. Steenbeck, T. Eick, K. Kirsch, Vacuum 58 (2000) 135.
[26] S.Y. Yang, W.L. Kuang, C.H. Ho, W.S. Tse, M.T. Lin, S.F. Lee, Y. Liou, Y.D. Yao, J. Magn. Magn. Mater. 226–230 (2001) 690.
[27] M. Sirena, N. Haberkorn, M. Granada, L.B. Steren, J. Guimpel, J. Magn. Magn. Mater. 272–276 (2004) 1171.
[28] Y.S. Du, B. Wang, T. Li, D.B. Yu, H. Yan, J. Magn. Magn. Mater. 297 (2006) 88.
[29] K.R. Lee, Y.J. Chung, J.H. Lee, J.S. Song, S. Park, Thin Solid Films 426 (2003) 205.
[30] D.R. Sahu, Appl. Surf. Sci. 255 (2008) 1870.
[31] K.X. Jin, S.G. Zhao, J. Tang, C.L. Chen, J. Alloys Compd. 476 (2009) 765.
[32] S.Y. Yang, W.L. Kuang, Y. Liou, W.S. Tse, S.F. Lee, Y.D. Yao, J. Magn. Magn. Mater. 268 (2004) 326.
[33] K.K. Choi, T. Taniyama, Y. Yamazaki, IEEE Trans. Magn. 35 (1999) 2844.
[34] H.L. Ju, H. Sohn, Solid State Commun. 102 (1997) 463.
[35] G.C. Xiong, Q. Li, H.L. Ju, S.N. Nao, L. Senapati, R.L. Greene, T. Venkatesan, Appl. Phys. Lett. 66 (1995) 1427.
[36] W. Prellier, A. Biswas, M. Rajeswari, T. Venkatasan, R.L. Greene, Appl. Phys. Lett. 75 (1999) 397.
[37] J.Q. Guo, H. Takeda, N.S. Kazama, J. Appl. Phys. 81 (1997) 7445.
[38] J. Dho, N.J. Hur, J. Appl. Phys. 94 (2003) 7670.
[39] M. Salvato, A. Vecchione, A. De Santis, F. Bibba, A.M. Cucolo, J. Appl. Phys. 97 (2005) 103712.
[40] A. Urushibara, Y. Moritoma, T. Arima, A. Asamitsu, G. Kido, Y. Tokur, Phys. Rev. B 51 (1995) 14103.
[41] P. Perna, L. Mechin, M.P. Chauvat, P. Ruterana, C. Simon, U.S. di Uccio, J. Phys.: Condens. Matter 21 (2009) 306005.
[42] D.R. Sahu, D.K. Mishra, J.-L. Huang, B.K. Roul, Physica B 396 (2007) 75.
[43] M. Sahana, T. Walter, K. Dorr, K.H. Muller, D. Eckert, K. Brand, J. Appl. Phys. 89 (2001) 6834.
[44] Y.M. Kang, H.J. Kim, S. Yoo, Appl. Phys. Lett. 95 (2009) 052510.
[45] A.K. Pradhan, D. Hunter, T. Williams, B. Lasley-Hunter, R. Bah, H. Mustafa, R. Rakhimov, J. Zhang, D.J. Sellmyer, E.E. Carpenter, D.R. Sahu, J.L. Huang, J. Appl. Phys. 103 (2008) 023914.
[46] U.S. diUccio, B. Davidson, R.D. Capua, F.M. Granozio, G. Pepe, P. Perna, A. Ruotolo, M. Salluzzo, J. Alloys Compd. 423 (2006) 228.
[47] B. Kim, D. Kwon, J.H. Song, Y. Hikita, B.G. Kim, H.Y. Hwang, Solid State Commun. 150 (2010) 598.
[48] I. Bergenti, V. Dediu, E. Arisi, M. Cavallini, F. Biscarini, C. Taliani, M.P. de Jong, C.L. Dennis, J.F. Gregg, M. Solzi, M. Natali, J. Magn. Magn. Mater. 312 (2007) 453.
[49] G.J. Chen, Y.H. Chang, H.W. Hsu, Mater. Sci. Eng. B 68 (1999) 104.
[50] X.W. Li, A. Gupta, G. Xiao, G.Q. Gong, Appl. Phys. Lett. 71 (1997) 1124.